Mass Shifter Mechanism for Small Rudderless Autonomous Underwater Vehicle

Min-Fan Ricky Lee, *member, RST,* and Yen-Chun Chen

***Abstract*—Underwater vehicles have been applied to underwater investigation and monitoring. Due to the introduction of a variety of new technologies, underwater vehicles are used for more long-term, routine, or dangerous tasks in deeper waters. To be suitable for deep underwater environments and long-lasting applications, the design without rudder or diving planes will simplify the control methods and enhance the leakproofness of underwater vehicles by reducing the gaps to install the moving parts such as rudders and diving planes. This paper propose a novel mass shifter mechanism for the motion of a small autonomous underwater vehicle. The new UV platform is equipped with two counterweights that move on fixed tracks. The yaw and pitch angles are changed by moving the two counterweights to the planned positions which change the center of gravity of underwater vehicle. A microcontroller is used to control the parts of this mass shifter mechanism inside the UV system. Algorithm and mechanism of the control system are addressed and the functions of all parts are clarified.**

***Index Terms*—Unmanned underwater vehicles, Autonomous systems, Mobile robots, Robot motion, Robot control**

I. Introduction

UNMANNED underwater vehicles becomes popular devices for investigating the conditions and substances below the water body in scientific and fishery applications due to the significant improvement by modern technology. In [1], it uses the innovative SyPRID sampler was used to collect plankton at a depth of about 6000 m. It can cooperate with the Sentry Autonomous Underwater Vehicle (AUV) to obtain a pair of large-volume plankton samples at a specified depth and measurement line. In [2], high-resolution autonomous sensors were equipped to AUV vehicle to routinely collect physical, chemical and biological data to identify bioluminescent dinoflagellates and zooplankton and investigate their living environment. See [3] for another example, AUVs were used for tracking marine animals tagged with individually coded acoustic transmitters and well demonstrated the advantages of AUVs in tracking underwater targets. The fluid of environments influences the hydrodynamic performance of an AUV. If your paper is intended for a conference, please contact your conference editor concerning acceptable word processor formats for your particular conference.

Since the UV operates underwater, the drag force of the environment fluid influence on the travel and steering of the UV. In [4], a two-phase computational fluid dynamics (CFD) method was applied on the evaluation of hydrodynamic performance of an axisymmetric AUV. The wave heights, Reynolds numbers and submerged depths of the AUV were influence the drag of AUV significantly. In [5], a mathematical model of hydrodynamics was applied on the calculation of the influence of wall in realizing the precise control and maneuverability of a complex-shaped underwater vehicles. In [6], it presents a method to save space for underwater glider in steering with a small pitch angle (SPA). For rudderless underwater gliders, steering under a SPA increases the steering angle and save the distance to complete an expected steering. The elevator and rudder mechanism will increase the design complexity of the leakprofness of the UV frame. Therefore, there are some studies on the use of rudderless designs to control the yaw and pitch angle of UV. In [7], the patent deploys at least two discharge nozzles for water jet flow as the main thrust of an underwater vehicle. It changed the balance of water flow cause the difference of thrust of two side. The change will produce the momentum on the UV to yaw the UV. In [8], a buoyancy control system was presented for underwater vehicles which mainly included a working chamber, piston and fluid. It controls the piston to move the fluid inside and outside to change center of gravity and change the pitch of UV. In [9], it presents a mass shifter mechanism for AUV. It can operate the changes of yaw and pitch angle by single set of mass shifter mechanism.

Underwater gliders are a category of underwater vehicles without external active propulsion systems. The trajectory study can help to evaluate the performance of underwater glider. In [10], the Glider Coordinated Control System (GCCS) using a complex glider model and a simple particle model for prediction and planning to steer a fleet of underwater gliders to a set of coordinated trajectories. In [11], This paper study the optimal path planning for UV assigned several targets by means of 3D Dubins curve. These path planning problems were modeled by the Multiple Traveling Sales Person (MTSP) and the Genetic Algorithm (GA) to get the optima. In [12], it presents a new design of mass shifter mechanism (MSM) inside an AUV platform. The AUV can perform horizontal motion and pitch angle and depth motion by changing the vehicle center of gravity.

II. Principle and Prototype

The center of mass in the underwater vehicle is aligned with three perpendicular axes of *X*, *Y* and *Z*. A right-handed coordinate system is used as in Fig. 1. The *X*-axis is parallel to the UV axial direction. The positive *X* direction is from the mass center of the UV directing to its nose. Surge is a conventional name used for a rotation around this axis. The *Y*-axis is perpendicular the UV's axial direction. The positive *Y* direction is from the mass center of the UV to the left side. A rotation around this axis is usually called sway. The *Z*-axis is perpendicular to both *X*-axis and *Y*-axis following a right-handed orientation system. The positive *Z* direction is from the mass center of the UV up to the above the UV.

Min-Fan Ricky Lee is with the Graduate Institute of Automation and Control, National Taiwan University of Science and Technology, Taipei, Taiwan (e-mail: rickylee@mail.ntust.edu.tw).

Yen-Chun Chen is with the Graduate Institute of Automation and Control, National Taiwan University of Science and Technology, Taipei, Taiwan.

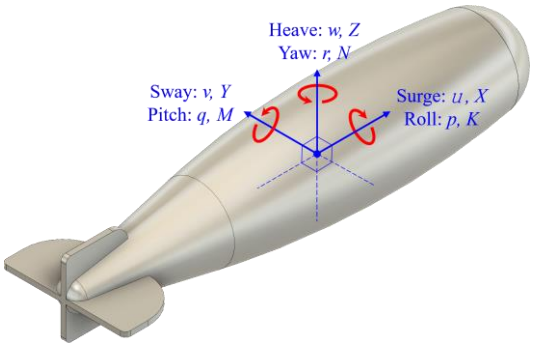

Fig. 1. Magnetization as a function of applied field. Note that

There is one mass shifter mechanism (MSM) system are deploy inside the underwater vehicle to achieve the steering and surfacing & diving process. The forces acting on the movable mass are the weight of the movable mass P, normal force F_N, total frictional force F_f, and force of the belt servo motor F_m, referring to [12]. In this Fig. 2, it is assumed that the movable mass is moving towards the stern of the vehicle with speed and the vehicle pitches up from horizontal at a pitch angle θ. Because friction always acts in a direction opposite the speed, the direction of total frictional force F_f, is towards the bow of the vehicle. The weight of the movable mass could be resolved into two components at right angles to each other, P_1 and P_2. P_1 is parallel to the mass shifter moving direction and P_2 is perpendicular to P_1. P_2 is balanced by the normal force F_N which is exerted on the movable mass by the screw shaft. The equation (1) describing the dynamics of the mass shifter mechanism is as follows:

$$m_e a_e = P_1 + F_f + F_m \qquad (1)$$

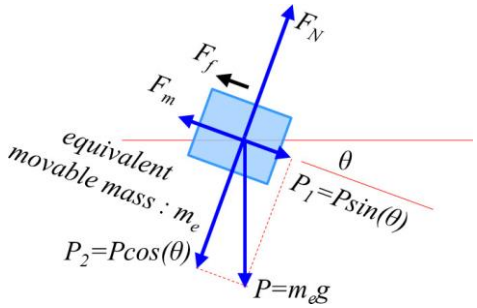

Fig. 2. Mass Shifter Mechanism (MSM).

III. Design Concept

A. Hardware Design Architecture

An underwater vehicle (UV) design concept is proposed in this study. The RoboLumilus with MSM are fabricated to verify this new concept for a rudderless design on underwater vehicle. There are five major potions in RoboLumilus including outer hull, motor and propeller, electronic control system, batteries, and mass shifter mechanism. The buoyancy of UV is designed slightly greater than its weight, therefore the UV will float to the water surface in the case of power lost.

In the study, a simple gyroscope and e-compass are deployed, but higher accuracy 9-axis gyroscope and e-compass they are recommended on next stage study for better feedback the status of underwater vehicle.

With a single propeller and mass shifter mechanism inside the UV hull, the UV can perform horizontal and vertical motion. It also controls pitch angle and depth motion with this inside MSM which changes the center of gravity of the UV. This mass shifter mechanism (MSM) is designed with two linear motion ball screws driven by step motors and two movable brass blocks as counterweights, shown in Fig. 3. When the two counterweights go forwards or backwards, the center of gravity of the whole underwater vehicle also shifts forwards or backwards and right or left. These shifts change the resultant forces and torque on underwater vehicle. The UV is propulsion of the thruster and will be propelled downward, or upward, or to right, or to right respectively. The resultant forces and torque of counterweights positions and UV motions are listed on Table I.

TABLE I
RESULTANT FORCES AND TORQUES FOR UV STATUS

UV Status	Resultant Direction	Torque Direction
Moving Ahead	+X	0
Turning right	+X	−Z
Turning left	+X	+Z
Diving	+X and −Z	+X
Surfacing	+X and −Z	−Z

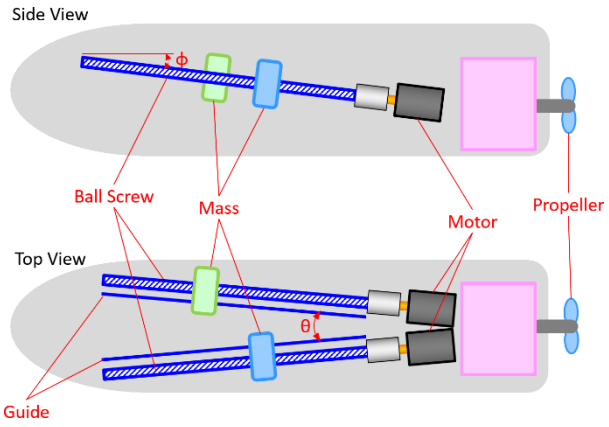

Fig. 3. Mass shifter mechanism (MSM) design.

B. MSM for yaw

Steering control algorithm is to achieve yaw angle. The UV design is to causes torque on the vehicle using the masses shift in steering process. The center of gravity (COG) will shift a distance d from original COG and perpendicular to the X axis. The equivalent driving force F still applies on the original COG and will cause a torque τ on the new COG. It will cause a steering force apply on the underwater vehicle. In Fig. 4, it is an example for the right turn and same rule but opposite masses moving for left turn. When an underwater vehicle steers under an MSM, one mass moves forward and another moves backward, the vertical angle will still keep the same.

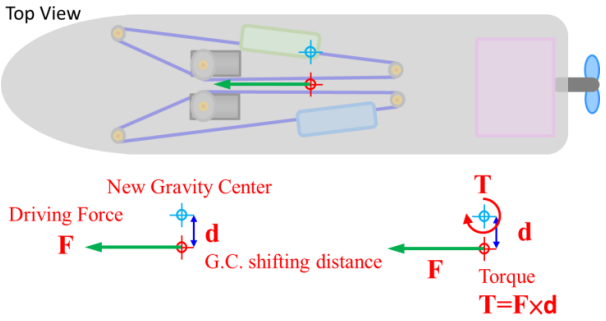

Fig. 4. Momentum for steering.

C. MSM for surfacing and diving

Surfacing and diving control algorithm is to change a resultant force on the *UV*. The forces acting on UV are as center of gravity (COG) will shift a distance d from original center of gravity and perpendicular to the *Y* axis from the natural status as Fig. 5-1. The equivalent driving force *F* and unbalance buoyance on the new COG cause a torque *T* on the new COG as in Fig. 6, the two massed moves forward together and the underwater vehicle bow will depress with an angle and underwater vehicle will diving. For surfacing, it is the similar action but different direction to move for MSM. In Fig. 7, the two massed moves backward together and the underwater vehicle bow will depress with an angle and underwater vehicle will diving. s an example for the right turn and same rule but opposite masses moving for left turn. When an underwater vehicle steers under an MSM, one mass moves forward and another moves backward, the vertical angle will still keep the same.

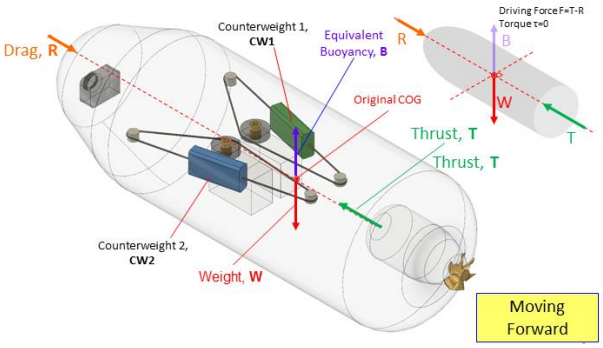

Fig. 5. MSM in Natural status.

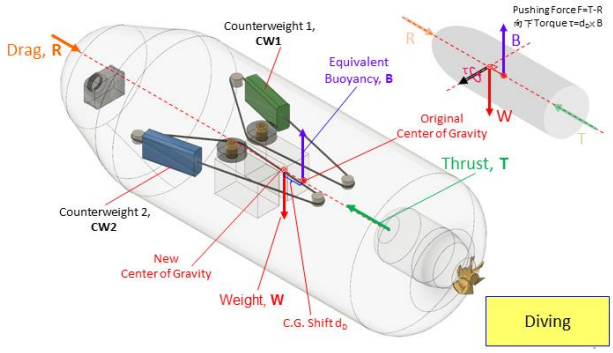

Fig. 6. MSM action for diving.

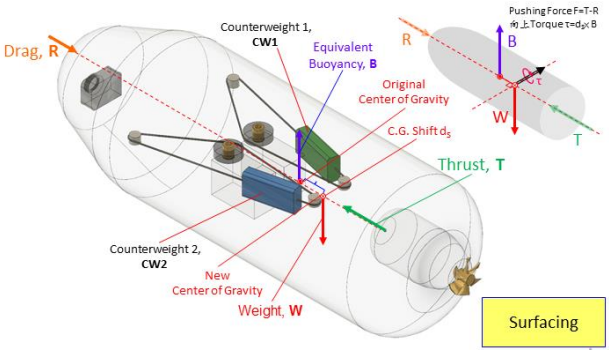

Fig. 7. MSM action for surfacing.

IV. Mechanical Architecture

A. Mass Shifter Mechanism on RoboLumilus

There are four major mechanical potions in RoboLumilus including outer hull, propulsion assembly, MSM, and Brass Chassis, as. Fig. 8.

The mass shifter mechanism is deployed in RoboLumilus, as Fig. 9. The couplings connect stepper motors and ball screws. The brass counterweights are fixed to spiral ball bearings and linear bearings. The ball screws and the linear guide rods are combined with the mass forming block on the T-slot aluminum frame via the brackets. There are two sets of symmetrical mass moving combinations in mass shifting mechanism are fitted on the brass chassis with an angle, and when the stepping motor rotates forward or reverse, the mass is advanced or retracted. Since the two mass moving combinations have an angle, when the mass moves one forward and the other moves backwards and the mass produces a near *Y* axis or away from *Y*, or the mass moves forward or backward at the same time, thereby making the system The movement of the center of mass before and after, the center of mass of the body changes.

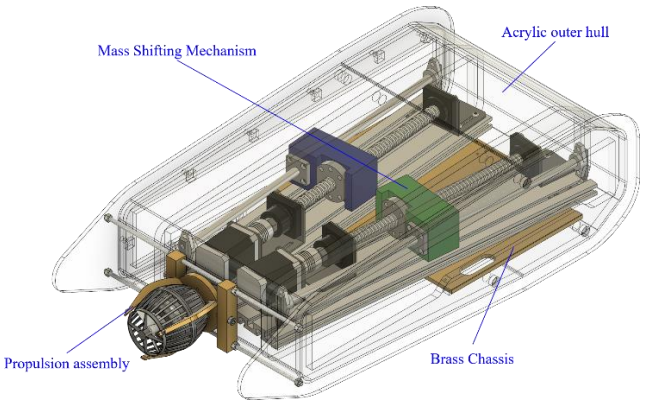

Fig. 8. Four major mechanical portions of RoboLumilus.

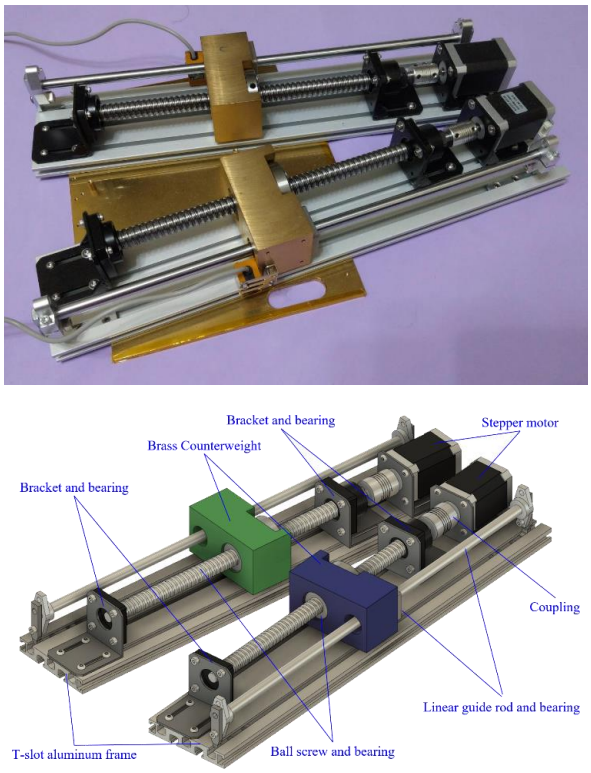

Fig. 9. Mass Shifter Mechanism of RoboLumilus (Top) Actual;(Bottom) CAD design.

B. Propulsion Assembly

In RoboLumilus, the propulsion assembly includes propeller, motor, and adjustable bracket, as Fig. 10(a) and 10(b). It controls the force of acting on RoboLumilus. To adjust the direction of the thrust T of the propeller to divide into forward and downward component forces, as in Fig. 11. The resultant of forward component force deducting the drag force *D* is net thrust to drive the RoboLumilus moving forward. The downward component force is approximately equal to the buoyancy *B* minus the gravity *W*. It keeps RoboLumilus travel under water after the diving process. To achieve this purpose, the adjustable brass bracket is used to adjust the motor and propeller, as Fig.6-1. The motor and propeller are screwed to the adjustable brass bracket. After adjusting the motor and propeller to an appropriate angle, fasten screw to fix the thruster direction.

From the impulse-momentum theorem states, the change in momentum of an object equals the impulse applied to it. The equation is as below.

$$F\Delta t = m\Delta v$$

C. Hull Design

For the view of fluid mechanics, the resistive force act opposite to an object moving inside fluid is called drag force. The drag force depends on velocity of object. The traditional expression of drag force FD is as below equation (1)

$$F_D = \frac{1}{2}\rho v^2 C_D A \qquad (1)$$

Where

F_D: the drag force

ρ: the fluid density

v: the velocity of the object relative to the fluid

A: the cross-sectional area of object

C_D: the dimension less number

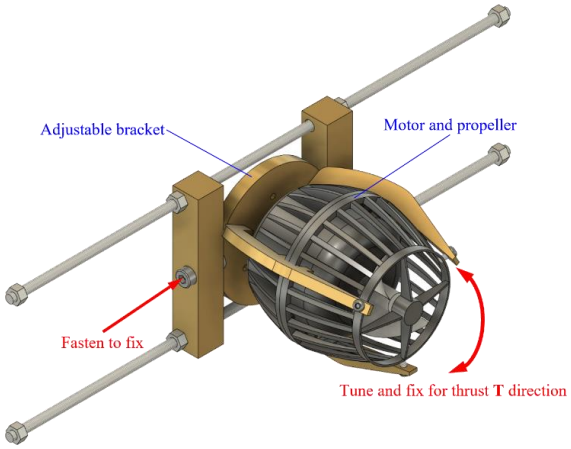

Fig. 10. (Top) Propeller and bracket; (Bottom) Adjustable propeller bracket.

The drag coefficient CD is a dimensionless number and depends on the shape of the object. The drag coefficient of object moving inside fluid is mainly related to skin friction and form drag. Referring to the drag coefficient of common shapes in Fig.12, the streamline design is with low drag. The hull of RoboLumilus is tried to close to streamline. Considering the manual

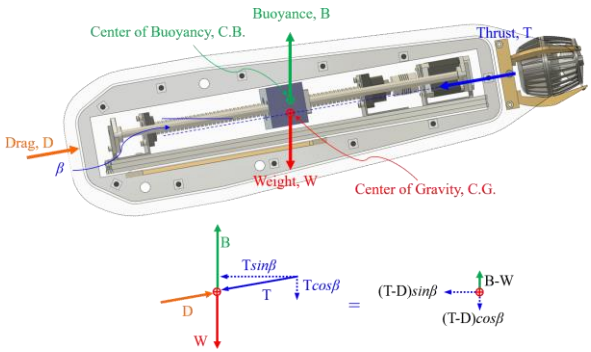

Fig. 11. Free-body diagram on RoboLumilus.

fabrication of acrylic hull, some planes are reserved for better manufacturing accuracy.

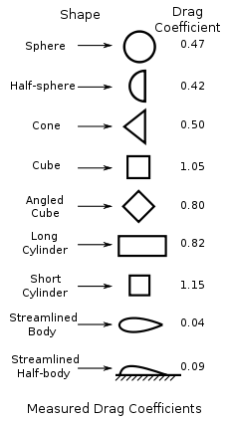

Fig. 12. Drag Coefficients for Reynolds number approximately 10^4 (Picture from https://en.wikipedia.org/wiki/Drag_coefficient).

Five pieces of laser-cut and calibrated acrylic spacers are designed to support the MSM and other auxiliary items that drive the mechanism, as in Fig.13.

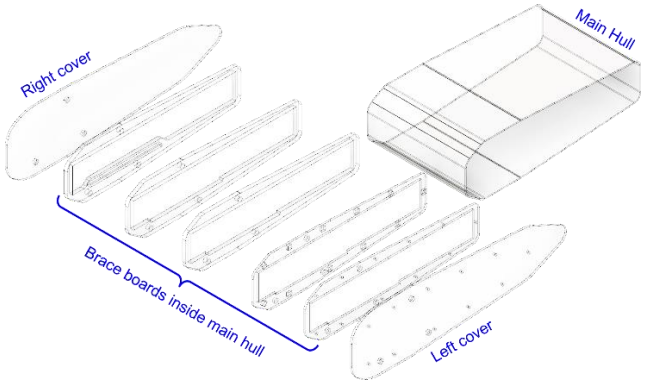

Fig. 13. Exploded-view drawing for acrylic.

Use the CAD software to create a 3D model of RoboLumilus and calculate the volume, as in Fig. 14. According to the Archimedes principle, buoyancy of an object completely or partially immersed in the rest liquid are subjected to the weight of volume the object displaces. Open the gravity of the fluid. Referring to Archimedes' law, the gravity of the object can be obtained as the gravity of the part of the fluid. The position of the buoyancy center is the position of the center of gravity of the fluid weight of the volume displaced by this

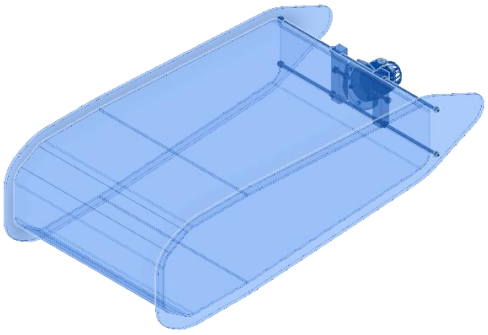

Fig. 14. Computer Simulated Volume of RoboLumilus.

object, and it is equivalent to the pressure difference results in a net upward force on the object. The forces of pressure on an object immersed in liquid are distributed to the object surface. According to the statics theory, all forces can be combined it to a net force buoyancy acting on the buoyancy center. The upward buoyancy force on an object acts through the center of buoyancy, being the geometric center of the displaced volume, as in Fig. 15. An object immersed in fluid is stable if it tends to restore itself to an equilibrium position when the center of gravity and center of buoyancy are collinear in *z* axis direction and former are below the later.

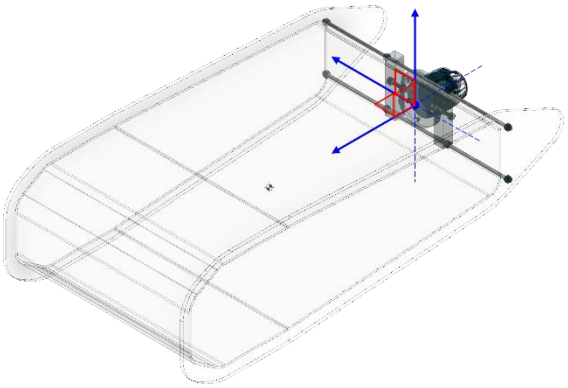

Fig. 15. Buoyancy center and coordinate system.

V. Control Method and Process

A. Control Concept

In this study, the feasibility of using this MSM as a motion control tool is verified. There are three portions of control circuit, including Instruction & Monitoring, Controller &

Sensors and Actuators. Instruction & Monitoring is used to instruct the RoboLumilus. Currently, a personal computer worked as a control console. It is connected to Arduino Micro control board on RoboLumilus via a USB CABLE. The Arduino Micro control board is the major part of the Controller & Sensors portion. Its I/O interface are connected to the limit switch for positioning and 9-axis IMU. Considering the perturbation in the water, the IMU is selected the product with Kalman filter function. The actuator portion is to execute the on and off actions of the controller. This portion includes driver

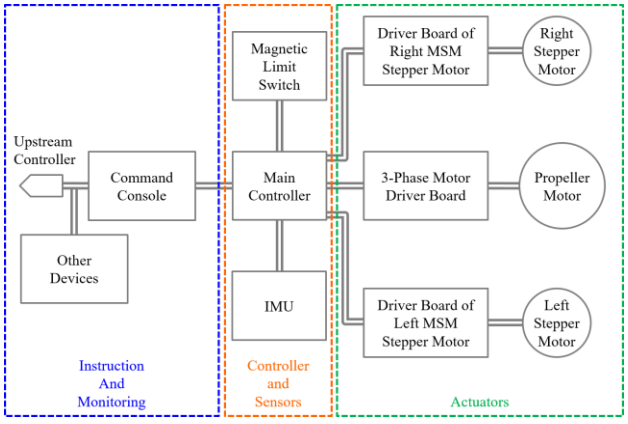

Fig. 16. Sensors installation for position detection.

boards and motors.

B. Electronic Circuit

The electronic circuit is divided into several parts, including the main controller, sensors, propulsion control, and stepper motor driver as shown in Fig. 17. In addition, there are also boost converter and buck converter circuits required for power sources from batteries. The device modules are used to save volume. The photographs of the entity are shown in Fig.18. Considering maintenance, each portions of the functions are separated and connected by plugs and receptacles with each other.

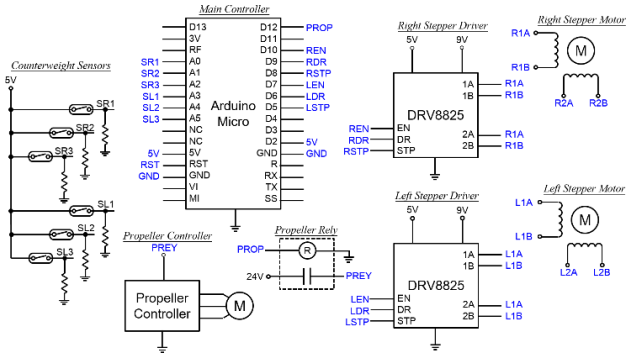

Fig. 17. Single-Board of Arduino Micro and peripherals.

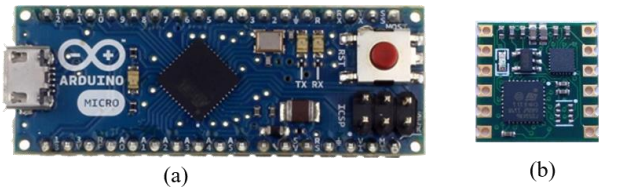

(a) (b)

(c) (d)

Fig. 18. Major components of electronic circuit (a) Arduino Micro controller board (b) 9-axis IMU (c) DRV8825 stepper motor (d) magnetic limit switch sensor.

C. Electronic Circuit

In order to move the counterweights to the proper positions, the sensors are equipped to detect the position of counterweights. In this design, the counterweights move to fixed position to transfer of the center of gravity. Therefore, the magnetic limit switches and the magnetic strip are used as the position indication, as shown in Fig. 19. Three magnetic limit switches were used, marked as SR1/SR2/SR3 and SL1/SL2/SL3 indicating the three magnetic limit switches on the right and left sides of MSM. SL1 and SR1 are used to detect the front end and back end. SL2/SL3 and SR2/SR3 are used to detect whether the counterweight is in the forward stroke or the rear stroke, as Fig. 20.

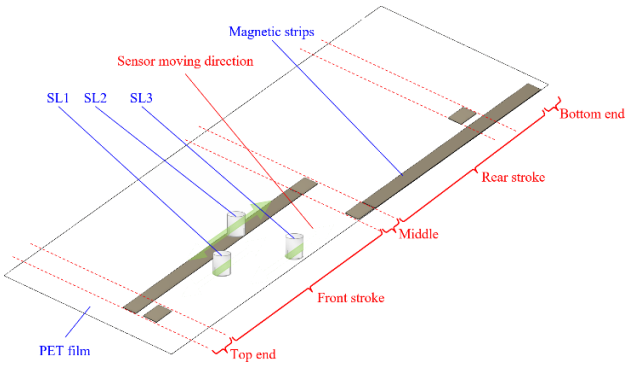

Fig. 19. magnetic strip on a PET fil.

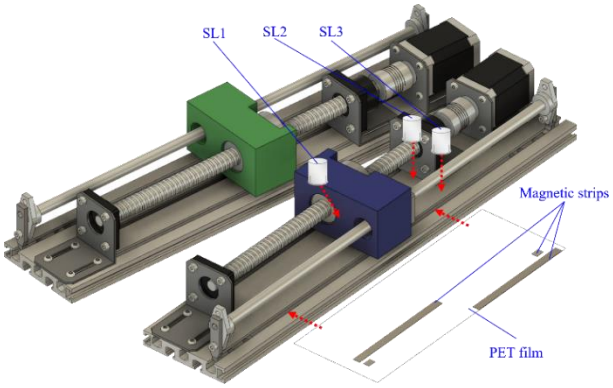

Fig. 20. Sensors installation.

Connect all the magnetic limit switches to the voltage signal source. When the magnetic limit switches move with the counterweight, the signals to controller change due to the corresponding positions magnetic strip, as shown in Fig. 16. These signals are connected to the I/O interface of the controller and the controller senses the counterweight positions. The controller will turn on and off the stepper motors used to drive the counterweight ball screws to locate the counterweights at correct positions. The excepted signals are as Table II.

TABLE II
SIGNAL LEVEL ON SENSOR FOR COUNTERWEIGHT POSITION

Position / Sensor	Top end	Front stroke	Middle	Rear stroke	Bottom end
SR1/SL1	1	0	0	0	1
SR2/SL2	1	1	0	0	0
SR3/SL3	0	0	0	1	1

D. Power Sources

RoboLumilus target to act as vehicle for long-term use under water, the chargeable batteries are used as the power source. The thruster and stepper motor have large current consumption requirements, so lithium iron phosphate battery

cells are selected as the entities of batteries.

The formula of lithium iron phosphate is LiFePO4, abbreviated as LFP. It is a kind of lithium ion battery. The lithium iron phosphate battery named after its positive electrode material is also called lithium-iron phosphate battery. It is characterized by no precious elements such as cobalt. The raw material price is low and phosphorus and iron are abundant in the earth's resources. There will be no supply problems. It has a working voltage of 3.3V with high discharge power, fast charging and long cycle life, and high stability in high temperature and high temperature environments. In this UV, two sets of four lithium iron phosphate batteries in parallel are used with a voltage of about 13.2V, as fig.21.

Fig. 21. Lithium Iron Phosphate Battery Assembly.

E. Program for System Control

In this study, we use Arduino Micro single boards as Fig. 18(a). "Arduino" is a product of the Arduino Company that makes open source hardware and software. The Arduino single-boards design are embedded various microprocessors. There are many versions, which can be selected according to the needs of control plans. The different versions are mainly equipped with different sets of digital and analog I/O pins and also other functional pins. Various expansion boards and sensors are designed to fit Arduino circuits. Arduino are usually with serial ports, including the universal serial bus (USB) on some models, which are used to upload programs from personal computers. The popular compliers usually use C/C++ programming language. At the beginning of the control program, reset all conditions of MSM and propulsion portions. Then the system waits the inputs of instruction to control RoboLumilus. We use manually input at this stage. If the instruction is for velocity, the Arduino controller adjust the revolution speed of motor for propeller. If the instruction is to change the direction, the controller sense the positions of counterweights. If the positions correctly match the setting, the controller do not send any signal to the drivers of stepper motor. If not, move to the position of counterweight to the target positions set for such direction. The program flow chart is as fig. 22.

F. Designs for Water Approval

In this study, we use two movable masses as counterweights to perform the yawing, diving and surfacing. The two movable masses position to controlling underwater are as below Table III. When UV keep the straight direction, the two massed should keep the original position where is aligned with the line from the right mass to the left mass and the original center of gravity is inside this line. The right mass will move forward and left mass will move backward to keep the *X* axis balance but enlarge the distance of d from new G. C. to the original COG The longer *d* will cause bigger torque to make the underwater turn right. to enhance the right roll momentum of the

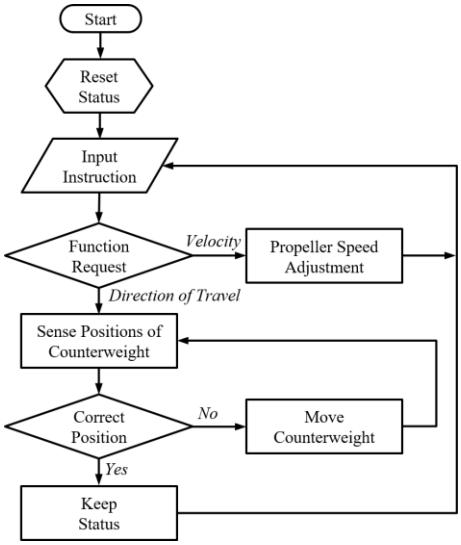

Fig. 22. Flow chart for control program.

underwater vehicle. The left turn also follows the same rule but opposite direction. The left mass will move forward and right mass will move backward to keep the X axis balance but enlarge the distance of d from new G. C. to the original COG this torque will cause the system turn left.

TABLE III
POSITIONS OF TWO MASSES FOR ROBOLUMILUS CONTROL

Vehicle Status	Mass #1 (Right)	Mass #2 (Left)	Torque
Move forward	Middle	Middle	0
Turn right	Top end	Bottom end	-Z
Turn left	Bottom end	Forward	+Z
Dive	Top end	Top end	+X
Surface	Bottom end	Bottom end	-X

VI. CONCLUSION

This paper presents a concept of mass shifter mechanism for an underwater vehicle. It is one of space-saving methods for UV motion control with simple mechanism instead of replace conventional rudder and elevator. It is not necessary to design any linking mechanism connecting the vehicle inside and outside and can enhance the seal degree for high water press in the deep water. A computer simulation is built to simulate the control algorithm. An analysis will be conducted to evaluate the effect of steering under an MSM initial condition including velocity, initial angle and different net buoyancies after complete the whole design of the real underwater vehicles.

RoboLumilus is a Prototype to verify the MSM method for UV control. For future development, it is recommended to optimize the MSM based on the same principle. So that the MSM can quickly move to the required positions and reduce the fluctuation of the hull during the movement. It is also recommended to change the positioning method of the counterweight from current discrete type to continuity type. In addition, the higher precision IMU can also increase the control stability of the UV. Besides, the controller and control logic can be integrated and enhance current ROV control method to AUV.

REFERENCES

[1] A. Billings, C. Kaiser, C.M. Young, L.S. Hiebert, E. Cole, K.S. Wagner, and L.V. Dover, "SyPRID sampler: A large-volume, high-resolution, autonomous, deep-ocean precision plankton sampling system," Deep Sea Research Part II: Topical Studies in Oceanography, vol. 137. pp. 297-306, Mar. 2017.

[2] M. Messié, I. Shulmanc, S. Martinid, S. Haddocka, "Using fluorescence and bioluminescence sensors to characterize auto- and heterotrophic plankton communities," Progress in Oceanography, vol. 171, pp. 76-92, Feb. 2019.

[3] T. Dodson, T. M. Grothues, J.H. Eiler, J.A. Dobarro, R. Shome, "Acoustic-telemetry payload control of an autonomous underwater vehicle for mapping tagged fish". Limnology and Oceangraphy-Methods. vol. 12. no. 11. pp. 760-772. Nov. 2018.

[4] W. Tian, B. Song, H. Ding, "Numerical research on the influence of surface waves on the hydrodynamic performance of an AUV". Ocean Engineering. vol. 14, pp. 373-386. April 2009. vol.183, pp. 40-56, Jul. 2019.

[5] Z.D. Li, et al., "Hydrodynamic calculation and analysis of a complex-shaped underwater robot based on computational fluid dynamics and prototype test". Advance in Mechanical Engineering. vol. 9, no. 11, Nov. 2017, Art. No. 1687814017734500.

[6] Y. S. Zhu, C. J. Yang, S. J. Wu, Q. LI, X. L. Xu, "A space-saving steering method for underwater gliders in lake monitoring," Frontiers of Information Technology & Electronic Engineering, vol. 16, No. 7, pp. 485-497, Mar. 2017.

[7] M.W. McBride and F.S. Archibald, "Propulsion of underwater vehicles using differential and vectored thrust," U.S. Patent US6 581 537 B2, Jun. 23, 2002.

[8] M.W. McBride and F.S. Archibald, "Buoyancy control systems and methods," U.S. Patent US 7 921 795B2, Apr. 12, 2011.

[9] N. H. Tran, H. S. Choi, J. H. Bae1, J. Y. Oh, and J. R. Cho, "Design, Control, and Implementation of a New AUV Platform with a Mass Shifter Mechanism," International Journal of Precision Engineering and Manufacturing," vol. 16, No. 7, pp. 1599-1608, June 2015.

[10] D.A. Paley, F. Zhang and N. E. Leonard, "Cooperative Control for Ocean Sampling: The Glider Coordinated Control System," IEEE Transactions on Control Systems Technology. vol. 16, pp. 735-744. Jul. 2008.

[11] W. Cai, M. Zhang, Y.R. Zheng, "Task Assignment and Path Planning for Multiple Autonomous Underwater Vehicles Using 3D Dubins Curves," Sensors. vol. 17, no.7, Jul. 2017, Art. no. 1607.

[12] N. H. Tran, H. S. Choi, J. H. Bae1, J. Y. Oh, and J. R. Cho, "Design, Control, and Implementation of a New AUV Platform with a Mass Shifter Mechanism," International Journal of Precision Engineering and Manufacturing," vol. 16, No. 7, pp. 1599-1608, June 2015.

Min-Fan Ricky Lee received the *M.Eng. degree* in *Department of Mechanical Engineering* from *Cornell University, NY, USA*, in *1991*, and *Ph.D. degree* in *Department of Agricultural and Biological Engineering* from *Cornell University, NY, USA*, in *1996*. He is currently an *Associate Professor* with the *Graduate Institute of Automation and Control, National Taiwan University of Science and Technology, Taiwan*. His current research interests and publications are in the areas of *Artificial Intelligence and Robot*.

Yen-Chun Chen received the *M.S. degree* in *Department of Agricultural Mechanical Engineering* from *National Chung Hsin University, Taiwan*, in *1995*. His current research interests and publications are in the areas of *Agricultural Automation* and *Autonomous Robot System*.